Supporting Information for "Market Potential for CO_2 Removal and Sequestration from Renewable Natural Gas Production in California"

Jun Wong Jonathan Santoso Marjorie Went Daniel Sanchez*

January 2022

Supporting Information: Additional details on methods, calculations, and results. Exact model formulation is included. 16 pages, 3 tables, 4 figures

*Wong: Kenneth C. Griffin Department of Economics. University of Chicago. 1126 E. 59th Street, Chicago, IL 60637, United States. Santoso and Went: Department of Chemical and Biomolecular Engineering. University of California, Berkeley. 201 Gilman Hall, University of California, Berkeley, CA 94720-1462, United States. Sanchez: Department of Environmental, Science, Policy, and Management. 130 Mulford Hall 3114, Berkeley, CA 94720-3114, United States. Corresponding author: sanchezd@berkeley.edu. Code and replication kit can be found on GitHub.

1 More on data development

1.1 Sequestration sites and costs

We filter the NATCARB saline aquifer database to only sequestration sites with nonurban layers using urban area definitions from (1) and the (2). We further filter the NATCARB database using a depth to basement of 1500m to ensure the safety of CO_2 sequestered. Depth to basement is obtained from the (3). We use a conservative measure of depth to basement (as opposed to 800m) to allow for the uncertainty of the policy directive regarding CCS in California. We filter the data available from Breunig et al. (4) to those flagged as suitable for anaerobic digestion. In particular, we do not consider the more lignin-rich feedstocks that are less prone to anaerobic digestion. While biogas from gasification is a studied and relatively mature technology, we constrain this paper to biogas from anaerobic digestion (5). The hand-collected data on existing anaerobic digesters are then geocoded using the Google Maps Place API (6).

We determine the sequestration storage costs following Sanchez et al. (7). In particular, saline aquifer storage and capacity and location are derived from NATCARB v1502 (8). Discussed above, we extend the approach in Sanchez et al. (7) by further filtering for depth to basement past 1500m and sequestration sites in non-urban areas. Storage costs are estimated for each 10km by 10km grids. The cost of site characterization is based on areal footprint, well drilling and completion, injection equipment, operating and maintenance costs, and monitoring and verification costs (9, 10). We estimate the capacity-weighted levelized cost of sequestration for each site using the following equation:

$$C_{seq} = (CRF \times \frac{C_{well,D\&C} + C_{well,equip} + C_{well,O\&M} + C_{seismic}}{q_{well,max}} + CRF \times \frac{C_{char}}{q_{annual}} + C_{mon}) \times Q_{normalized} \tag{1}$$

where
C_{seq} = levelized cost of CO_2 ($/ton)
CRF = capital recovery factor $C_{well,D\&C}$ = cost of drilling and completion
$C_{well,equip}$ = cost of well equipment
$C_{well,O\&M}$ = cost of well operation and maintenance
$C_{seismic}$ = cost of seismic assessment and monitoring
C_{char} = site characterization cost
C_{mon} = monitoring and verification cost
$q_{well,max}$ = maximum well injection rate
q_{annual} = annual injection volume
$Q_{normalized}$ = normalized saline aquifer capacity

The maximum well injection rate is asssumed to be 1 $MtCO_2$/y. We update the cost to 2018 US dollars using the IHS Upstream Capital Cost Index. We estimate the cost of seismic assessment and monitoring from C2SAFE. In particular, seismic assessment costs $160,000/km^2 of site area, and a constant 10 percent of total seismic cost for processing field data. Note that the characterization costs depend on the size of the aerial footprint, estimating as the following (11):

$$C_{char} = C_{areal,char} \times \lambda_c \times q_{annual} \times \frac{t}{\Psi \times b \times \lambda_w} \tag{2}$$

where
$C_{areal,char}$ = specific site characterization costs
q_{annual} = annual injection volume (at reservoir conditions)
λ_c = phase mobility of CO_2[1]
λ_w = phase mobility of brine
t = period of injection
b = CO_2 layer thickness
Ψ = porosity

[1]The phase mobility is the ratio of relative permeability to fluid viscosity

We estimate the physical properties needed for CO_2 and brine phase mobilities using Chung et al. (12) and Batzle and Wang (13), respectively. We include a \$52 million per site to account for development costs based on McCollum and Ogden (14). We assume a cost of monitoring and verification of \$0.1/tCO_2.

1.2 Digester Cost Estimation

We linearize the cost functions obtained from the literature. Specifically, we estimate the piecewise linear functions of the digester and upgrading cost functions in Parker et al. (15), compression and pumping cost in McCollum and Ogden (14), and carbon dioxide capture cost in Psarras et al. (16). Piecewise estimating non-linear functions allows us to better capture the economies of scale associated with CCS systems and stay within the framework of linear optimization. This reduces the model complexity and computational load while still approximating the importance of scale in CCS systems. We employ the cost model in Psarras et al. (16) to estimate the cost of CO_2 capture, assuming a 90% capture rate and 80.7% CO_2 concentration. Table S1 below lists the costs associated with each component.

For anaerobic digester costs, capacity is defined as kilotons per year. RNG Flow in the biogas upgrading and RNG compression and injection costs are measured in mmbtu per hour. For CO_2 capture, we present the levelized cost of capture (measured as \$/tCO_2). The capture rate is assumed to be 90%, concentration is assumed to be 98%, and the flow rate is measured as tonnes per day. In the cost function for CO_2 compression, m_{train} denotes the CO_2 mass flow rate through each compressor train measured in kg per second: $m_{train} = \frac{1{,}000 \times m}{24 \times 3{,}600 \times N_{train}}$ where m is the CO_2 mass flow rate to be transported to the injection site measured in tonnes per day. We assume that N_{train}, the number of compressor train, is one. We incur CO_2 compression costs twice: we compress the CO_2 once up to 1.7 MPa for transport, and again to 15 MPa at the sequestration site for injection. Thus, $P_{\text{initial}} = 0.1$ MPa and $P_{\text{final}} = 1.7$ MPa for the first round of compression, and subsequently $P_{\text{initial}} = 1.7$ MPa and $P_{\text{final}} = 15$ MPa for the second round of compression. The O&M cost of CO_2 compression includes both the maintenance cost of the compression equipment and the electricity cost. W_s represents the work required to compress CO_2 up to a certain pressure: $W_i = \sum_{s=1}^{5} \frac{1000}{24 \times 3600} \frac{m Z_s R T_{in}}{M \eta_{is}} \frac{k_s}{k_s - 1} [(\frac{P_{\text{cutoff}}}{P_{\text{initial}}}^{1/N_{\text{stage}}})^{\frac{k_s - 1}{k_s}} - 1]$. Here, R is the gas constant in kJ per kmol-K; T_{in} is the CO_2 temperature at compressor inlet in K, η_{is} is the isentropic efficiency of the compressor; M is the molecular weight of CO_2 in kg/kmol; Z_s is the average CO_2 compressibility for each individual stage; N_{stage} is the number of compression stages, assumed to be 5; k_s s the average ratio of specific heats of CO_2 for each stage. Each stage has different values for Z_s and k_s, but all other values are constant across the stages. CF denotes the capacity factor. Both the capital and operating costs of CO_2 pumping depend on W_p, defined as: $W_p = \frac{1000 \times 10}{24 \times 36} \frac{m(P_{\text{final}} - P_{\text{cutoff}})}{\rho \eta_p}$, where ρ is the density of CO_2 during pumping in kg/m^3; η_p is the efficiency of the pump. We do not make any assumptions on the capital costs of building a landfill gas collector since we restrict inputs to landfills with existing collectors. The landfill gas flow in the O&M cost is measured in standard cubic feet per minute. For both biomass and CO_2 transport, roundtrip duration is measured in hours and roundtrip distance is measured in miles. A truckload is defined as 25 wet tons for biomass transport and feedstock weight is measured in wet tons. For CO_2 transport, a truckload is defined as 25.67 tons of CO_2 compressed to 1.7 MPa.

Table S1: Summary of Cost Functions

	Functional Form	Source
Anaerobic Digester		
Capital Cost	$2,508,900 \times \sqrt{\frac{\text{Capacity}}{1000}}$	Parker et al. (15)
O&M Cost	$162,775 \times \text{Capacity}^{0.6}$	Parker et al. (15)
Biogas Upgrading		
Capital Cost	$1,064,800 \times \text{RNG Flow}^{0.48}$	Parker et al. (15)
O&M Cost	$74,950 \times \text{RNG Flow}^{0.69}$	Parker et al. (15)
RNG Compression & Injection		
Capital Cost	$615,750 \times \text{RNG Flow}^{0.42}$	Parker et al. (15)
O&M Cost	$28,425 \times \text{RNG Flow}^{0.35}$	Parker et al. (15)
CO_2 Capture		
Levelized Cost	$87.18 - 0.27 \times$ Capture Rate $- 86.84 \times$ Concentration $- 0.0006 \times$ Flow Rate	Psarras et al. (16)
CO_2 Compression		
Capital Cost	$m_{\text{train}} N_{\text{train}} \left[130,000 \times (m_{\text{train}})^{-0.71} + 1,400,000 \times (m_{\text{train}})^{-0.60} \ln(\frac{P_{\text{cutoff}}}{P_{\text{initial}}})\right]$	McCollum and Ogden (14)
O&M Cost	Capital Cost $\times 0.04 +$ Price $\times W_i \times CF \times 24 \times 365$	McCollum and Ogden (14)
CO_2 Pumping		
Capital Cost	$1,110,000 \times \frac{W_p}{1,000} + 70,000$	McCollum and Ogden (14)
O&M Cost	Capital Cost $\times 0.04 +$ Price $\times W_p \times CF \times 24 \times 365$	McCollum and Ogden (14)
Landfill Gas Collector		
Capital Cost	Presumed Built	
O&M Cost	$20 \times$ Landfill Gas Flow	Davis (17)
Biomass Transport		
Total Cost	$(26.11 \times$ Roundtrip duration $+ 1.08 \times$ Roundtrip distance$) \times$ Truckload $+ 4.50 \times$ Feedstock weight	Tittmann et al. (18)
CO_2 Transport		
Total Cost	$(18.31 \times$ Roundtrip duration $+ 0.80 \times$ Roundtrip distance$) \times$ Truckload	Psarras et al. (16)

1.3 Biogas yields

While we use the biogas yields in Li et al. (19) at baseline, we also survey the literature for a broad range of experimental biogas yields for sensitivity analysis. See Table S2 for the range of biogas yields considered and sources surveyed. In addition, we adopt the predictive biogas yield model from Escalante et al. (20) to supplement the literature values. We consider six independent variables: cellulose, hemicellulose, and lignin weight percentage; C:N ratio; and volatile and total solids percentage and the inoculum to substrate ratio. Table S3 panel A, presents coefficients for each predictive variable and panel B presents the estimated biogas yields for select feedstocks.

Table S2: Literature Biogas Yield (mL/g VS)

Feedstock	Min	Max
Manure	51	295
Crop Waste	49	390
Food Waste	180	540
Green Waste	180	540
Grease	648	811

Note: This table shows the range of biogas yields in the surveyed literature.

Table S3: Biogas Yield Prediction Model Coefficient

Panel A: Model Coefficients	
Variable	Coefficient
Cellulose	0.3445
Hemicellulose	0.0001
Lignin	-0.0001
C:N ratio	-0.0002
Percent Volatile Solids	-0.0040
Percent Total Solids	0.0012
Inoculum:Substrate ratio	-0.00002

Panel B: Average Estimated Yields (mL/g VS)	
Feedstock	Biogas Yield
Crop Residues	181.96
Food Waste	328.78
Manure	324.32

Note: This table shows the estimation of biogas yield following the method in Escalante et al. (20).

Unsurprisingly, Figure S1 shows that CH_4 and CO_2 output is the most sensitive to biogas yield asumptions. Under optimistic biogas yield assumptions, over 150 PJ of RNG is produced and 6 million tons of CO2 is sequestered at baseline policy support. Using more pessimistic biogas yield assumptions, only 40 PJ of RNG is produced and 1.5 million tons of CO2 sequestered. Despite this, biogas yield has little effect on profits in the model, with policy drivers such as LCFS and RFS driving most of the variation.

Figure S1: Sensitivity Analysis

(a) CH_4 Sensitivity

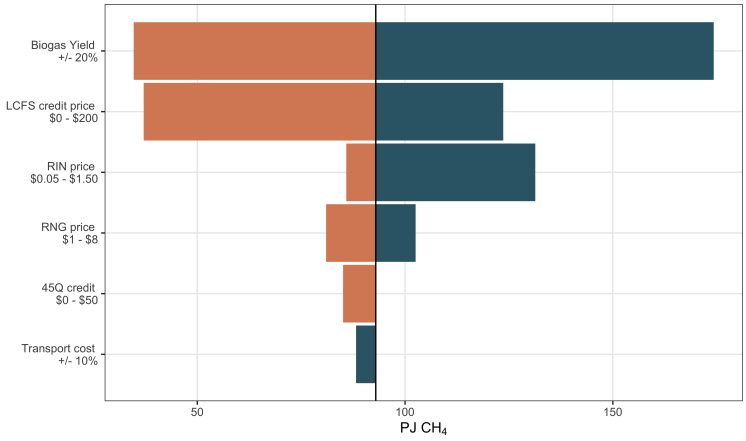

(b) CO_2 Sensitivity

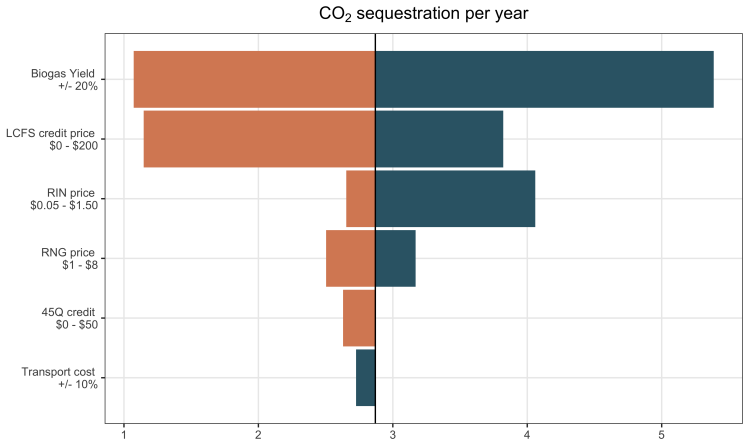

Note: Parametric sensitivity analysis of yearly (a) CH4 production and (b) CO_2 sequestration. We vary biogas yield, LCFS price, RIN credit price, RNG price, 45Q credits, and transport cost. Average profits are rarely fall below the baseline \$12/GJ, but can reach as high as \$37/GJ when RFS prices are at their highest.

This discussion on biogas yield requires two caveats: this model aggregates feedstock types into broad categories. Biogas yield varies within the broad categories presented in the paper, and considering the average biogas yield for all subtypes of biomass residues masks the variation in feedstock subtype availability across regions. In particular, agricultural production is relatively segregated in California: while Fresno primarily produce almonds and tomatoes, neighboring Tulare leads in orange production (21). The different climate in California implies that there will be important regional differences in available crop residues. Breunig et al. (4) provides more detail on the geographic (and temporal) variation in biomass residues across California. Second, special attention needs to be paid to codigesting facilities. In particular, while codigestion have the potential to further increase the biogas yield, it is also possible that biogas yield could be dampened due to an inappropriate mixture of feedstocks. In this paper, we assume that feedstocks are mixed homogenously, and their respective biogas yields aggregate linearly.

1.4 Carbon Intensity

We reference the temporary carbon intensity of CNG by feedstock input as estimated by the California Air Resources Board (22). Table S4 reproduces these estimates. These characterize the lifecycle carbon

intensity of the RNG produced but **excludes the additional CO_2 sequestration and the associated process emissions of sequestering the CO_2**. As with biogas yields, we assume that the carbon intensities of the produced RNG is proportional to the share of the feedstocks used. Thus, the carbon intensity of RNG produced from codigestion will be a weighted average of the carbon intensities of the RNG produced from these individual feedstocks. The system boundary of the CARB-estimated carbon intensities are "well-to-wheels," implying that it includes feedstock transport, production, and ultimate usage of the fuel. It also accounts for counterfactual usage of the feedstock (left to landfills or to flare). For the purposes of calculating additional LCFS credits, we supplement these carbon intensities by accounting for the additional CO_2 sequestered and its associated process emissions. We do so by first accounting for the electricity emissions associated with CO_2 compression and pumping, transport emissions for the CO_2, and the sequestered CO_2. We assume that the system uses California grid electricity with carbon intensity equal to the average California mix in 2018 (23). We also assume that the CO_2 transport incurs an emissions factor of 161.8 gCO_2/ton-mile (24).

Table S4: Carbon Intensity of RNG by Feedstock Input

Feedstock	Carbon Intensity
Crop Residue	45 gCO_2e/MJ
Food Waste	45 gCO_2e/MJ
Grease	45 gCO_2e/MJ
Green Waste	45 gCO_2e/MJ
Landfill Gas	70 gCO_2e/MJ
Manure	-150 gCO_2e/MJ
Wastewater	45 gCO_2e/MJ

2 Biogas upgrading technologies

In this paper, we consider pressure swing adsorption (PSA) for biogas upgrading. There are other technologies available, with varying CH_4 and CO_2 purity and costs. We briefly discuss the implications of various technologies while we direct interested readers to Sun et al. (25) and Ong et al. (26) for an in-depth overview of biogas upgrading technologies. Among the various biogas upgrading technologies, water scrubbing, pressure swing adsorption, and chemical scrubbing are the most commonly applied technologies (26). In particular, PSA is relatively inexpensive and is widely practiced. It also requires no heat demand and low energy use. It's applicability to small capacities is especially helpful in our context. Water scrubbing is similarly inexpensive, but it requires large amounts of water to operate and requires biomethane drying. Chemical scrubbing, unlike PSA and water scrubbing, yields higher methane content, but it is relatively more expensive and difficult to operate. The costs of upgrading technologies are varied, but PSA is consistently one of the lower cost options across case studies. The choice of biogas upgrading technology could be consequential to the model outcomes. In particular, what is the trade off between the purity of CH_4 and CO_2 streams, the energetic content of the resulting natural gas, and the cost of technology? However, the results in Figure S2 suggests that the upgrading costs are relatively small compared to digester cost or CCS-related costs.

3 Additional results

Figure S3 shows that at baseline, a majority of available feedstocks are utilized, except for food waste. The current policy incentive is sufficient to spark a profitable, carbon negative, waste management program in California. However, the relatively small utilization of food waste points to the importance of transportation costs. However, the outsized profitability of the RNG-CCS system indicates that it is possible to further manage food waste in a similar manner while maintaining a profitable system.

Figure S2: Cost and Revenues

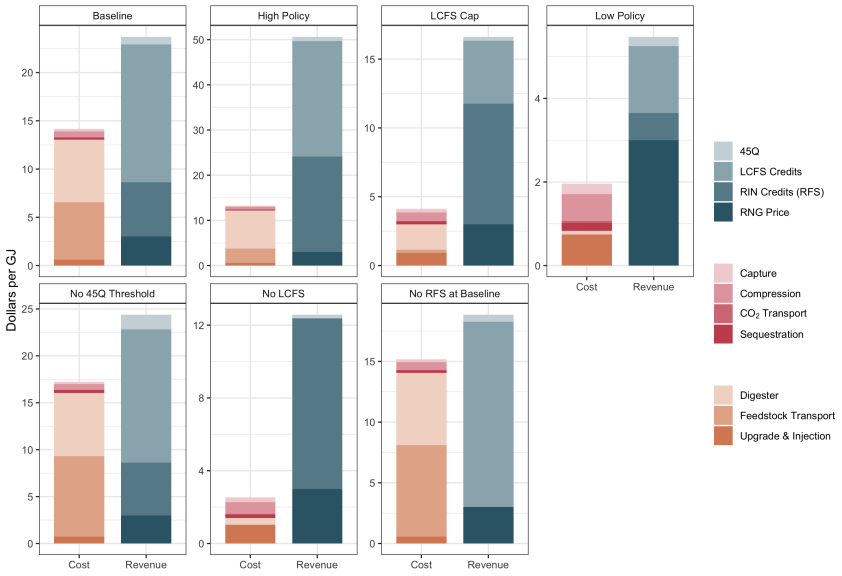

Note: Costs and revenues ($/ GJ) for RNG-CCS system for various policy scenarios. Costs are separated into two technology categories: CCS-related (red) and biomass processing-related (orange). Across all scenarios, CCS-related costs are a small fraction of total costs. Revenues from the LCFS make up a large share of revenue across all scenarios.

Figure S3: Feedstock utilization

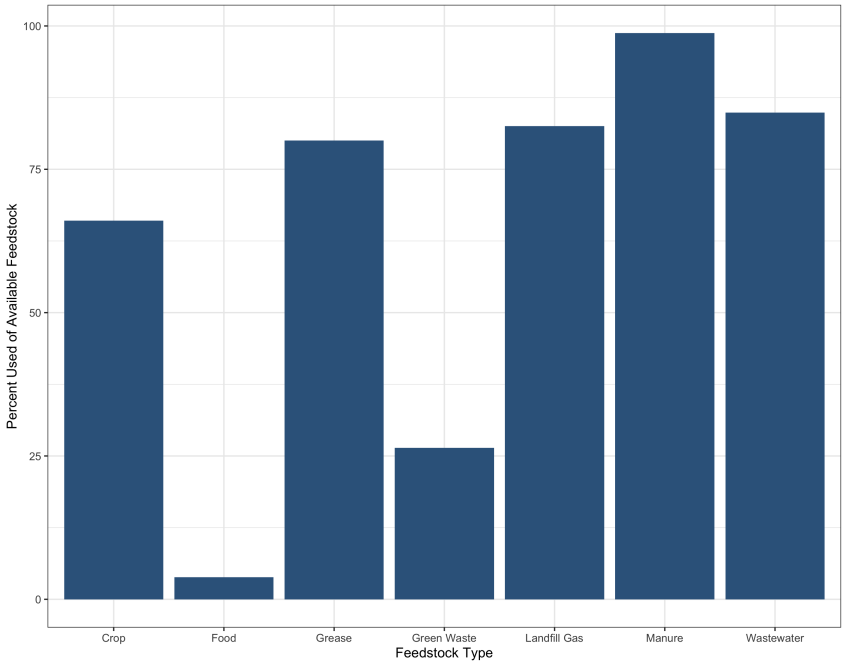

Note: This figure shows the percent of feedstock utilized at the baseline scenario. Wastewater is taken as a percentage of *active* facilities, not *all* facilities.

Figure S4 shows the geographical distribution of facility level cost at baseline. We see the landfills are consistently less expensive than codigesters, this is because landfills lack the need for an anaerobic digester. There is a lower-cost agglomeration in the greater Los Angeles area, while Imperial county sees a higher-cost cluster. Furthermore, cost is directly correlated with facility size—the smallest facilities are

Figure S4: Levelized Cost

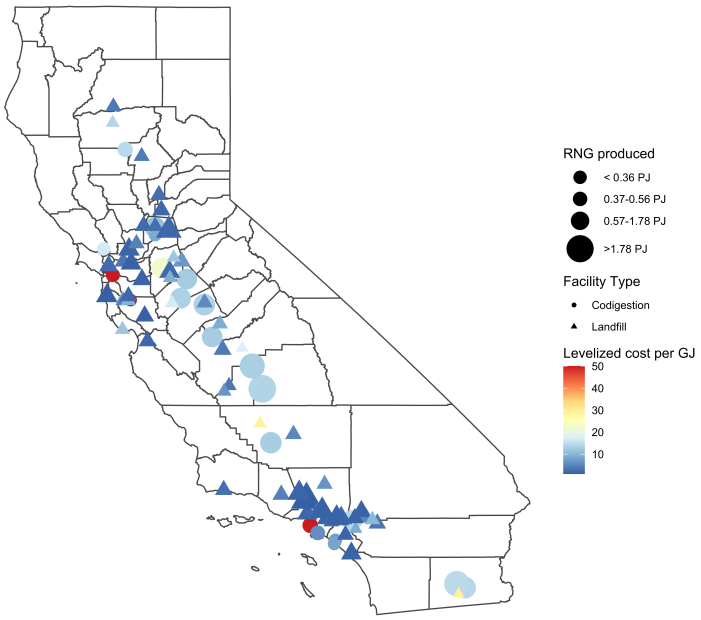

Note: This figure maps the levelized cost per GJ of RNG for each facility.

the most expensive (on a dollars-per-GJ basis). Note that such an uneven distribution of levelized cost across regions and facilities is only possible through a global optimization. Whereas a local optimization problem might see a significant decline in system size.

4 Model Formulation

4.1 Notation

Sets are as follows:

f	Facilities
$l \in f$	Landfills, a subset of facilities
$c \in f$	Codigesters, a subset of facilities
t	Feedstock type
$g \in t$	Landfill gas, a subset of feedstock type
$s \in t$	Set of codigestion types, subset of feedstock type
	$s = \{\text{Wastewater, Crop, Manure, MSW}\}$
i	Sequestration sites
s	Feedstock source
(s, f)	Feedstock source and facility pairs under 50 miles
(f, i)	Facility and sequestration site pairs under 50 miles

Parameters are as follows:

Facilities	
pipe_fc_f	RNG pipeline fixed cost at facility f
pipe_vc_f	RNG pipeline variable cost at facility f
lmop_l	Landfill collecting variable cost at landfill l
Sequestration sites	
injection_fc_i	CO_2 injection fixed cost at sequestration site i
injection_vc_i	CO_2 injection variable cost at sequestration site i
capacity_i	Sequestration site storage capacity at sequestration site i
seismic_i	3-D seismic survey cost at sequestration site i
Type	
ts_t	Total solids % of feedstock type t
vs_t	Volatile solids % of feedstock type t
ton_t	Conversion to ton of feedstock type t
biogas_yield_t	Biogas yield of feedstock type t
c_intensity_t	Carbon intensity of resultant RNG from feedstock type t
Feedstock source & type	
$\text{supply}_{s,t}$	Feedstock quantity at source s of type t
Valid source → facility pairs	
$\text{fs\_dist}_{s,f}$	Road distance between feedstock at location s and facility f
$\text{fs\_time}_{s,f}$	Travel duration between feedstock at location s and facility f
$\text{per\_ton}_{s,f}$	Per-ton cost from location s to facility f
Valid facility → sequestration site pairs	
$\text{rs\_dist}_{f,i}$	Road distance between facility f and sequestration site i
$\text{rs\_time}_{f,i}$	Travel duration between facility f and sequestration site i

Scalars are as follows:

Cost (in 2019 $)	
ad_fc_int	AD fixed cost intercept
ad_fc_slope$_1$	AD fixed cost slope below threshold
ad_fc_slope$_2$	AD fixed cost slope above threshold
ad_vc_int	AD variable cost intercept
ad_vc_slope$_1$	AD variable cost slope below threshold
ad_vc_slope$_2$	AD variable cost slope above threshold
up_fc_int	Biogas upgrading fixed cost intercept
up_fc_slope$_1$	Biogas upgrading fixed cost slope below threshold
up_fc_slope$_2$	Biogas upgrading fixed cost slope above threshold
up_vc_int	Biogas upgrading variable cost intercept
up_vc_slope$_1$	Biogas upgrading variable cost slope below threshold
up_vc_slope$_2$	Biogas upgrading variable cost slope above threshold
inj_fc_int	RNG injection fixed cost intercept
inj_fc_slope$_1$	RNG injection fixed cost slope below threshold
inj_fc_slope$_2$	RNG injection fixed cost slope above threshold
inj_vc_int	RNG injection variable cost intercept
inj_vc_slope$_1$	RNG injection variable cost slope below threshold
inj_vc_slope$_2$	RNG injection variable cost slope above threshold
comp_fc_int$_a$	CO_2 compression to transporting pressure fixed cost intercept
comp_fc_slope$_{a1}$	CO_2 compression to transporting pressure fixed cost slope below threshold
comp_fc_slope$_{a2}$	CO_2 compression to transporting pressure fixed cost slope above threshold
comp_vc_int$_a$	CO_2 compression to transporting pressure variable cost intercept
comp_vc_slope$_{a1}$	CO_2 compression to transporting pressure variable cost slope below threshold
comp_vc_slope$_{a2}$	CO_2 compression to transporting pressure variable cost slope above threshold
comp_fc_int$_b$	CO_2 compression to sequestration pressure fixed cost intercept
comp_fc_slope$_{b1}$	CO_2 compression to sequestration pressure fixed cost slope below threshold
comp_fc_slope$_{b2}$	CO_2 compression to sequestration pressure fixed cost slope above threshold
comp_vc_int$_b$	CO_2 compression to sequestration pressure variable cost intercept
comp_vc_slope$_{b1}$	CO_2 compression to sequestration pressure variable cost slope below threshold
comp_vc_slope$_{b2}$	CO_2 compression to sequestration pressure variable cost slope above threshold
cap_fc_int	CO_2 capture fixed cost intercept
cap_fc_slope$_1$	CO_2 capture fixed cost slope below threshold
cap_fc_slope$_2$	CO_2 capture fixed cost slope above threshold
cap_vc_int	CO_2 capture variable cost intercept
cap_vc_slope$_1$	CO_2 capture variable cost slope below threshold
cap_vc_slope$_2$	CO_2 capture variable cost slope above threshold
monitoring	CO_2 storage monitoring cost
fs_mi	Feedstock transport cost per mile
fs_hr	Feedstock transport cost per hour
rs_mi	CO_2 transport cost per mile
rs_hr	CO_2 transport cost per hour
Revenues ($/mmbtu)	
lcfs	LCFS credit price
d5	RIN D5 credit price
cellulosic_waiver	Cellulosic waiver price
45q	45Q tax credit
rng	RNG price
Other assumptions	
ch4_yield	CH_4 volume percentage in biogas
baseline_ci	Baseline carbon intensity of RNG
irr	Internal rate of return
life	Project lifetime (years)
crf	Capital Recovery Factor = $\frac{\text{irr}\times(1+\text{irr})^{\text{life}}}{(1+\text{irr})^{\text{life}}-1}$
electricity	Grid electricity carbon intensity
transport	Transport emissions
compression$_a$	CO_2 compression work to transporting pressure
compression$_b$	CO_2 compression work to sequestration pressure
co2_truckload	CO_2 transport truck capacity
fs_truckload	Feedstock transport truck capacity

Decision variables are as follows:

ad_f	Binary if facility f is active
seq_i	Binary if sequestration site i is active
$\text{q\_feed}_{s,f,t}$	Quantity of feedstock from source s of type t delivered to facility f
q_feedf_f	Total quantity of feedstock used at facility f $= \sum_{s,t} \text{q\_feed}_{s,f,t}$
q_feedf_nowwtp_f	Total quantity of feedstock used at facility f, excluding wastewater $= \sum_{s,t} \text{q\_feed}_{s,f,t} - \text{q\_feed}_{s,f,t=\text{wastewater}} \times \text{ton}_{t=\text{wastewater}}$
$\text{q\_ch4}_{t,f}$	Quantity of CH_4 from feedstock type t at facility f $= \sum_s \text{q\_feed}_{s,f,t} \times \text{ts}_t \times \text{vs}_t \times \text{biogas\_yield}_t \times \text{ch4\_yield}$
q_ch4f_f	Quantity of CH_4 produced at facility f $\sum_t \text{q\_ch4}_{t,f}$
q_captf_f	Quantity of CO_2 captured at facility f $= \sum_{s,t} \text{q\_feed}_{s,f,t} \times \text{ts}_t \times \text{vs}_t \times \text{biogas\_yield}_t \times (1 - \text{ch4\_yield})$
q_co2seq_i	Quantity of CO_2 sequestered at sequestration site i
$\text{q\_co2trans}_{f,i}$	Quantity of CO_2 transported from facility f to sequestration site i

4.2 Model

Objective Function. We aim to minimize net cost over the project lifetime:

$$\min \text{net cost} = \text{life} \times (\text{total cost} - \text{total revenue}) \tag{3}$$

where total cost is defined as:

$$\begin{aligned}
\text{total cost} = & \sum_c \Big\{ (\text{ad}_c \times (\sum_{i=1}^{n} \vec{\mathbf{Intc}}_i) + \\
& \vec{\mathbf{ad_fc}} \times \text{q_feedf_nowwtp}_c + \vec{\mathbf{ad_vc}} \times \text{q_feedf}_c + \\
& \vec{\mathbf{up_inj}} \times \text{q_ch4f}_c + \vec{\mathbf{comp_capt}} \times \text{q_captf}_c + \\
& \text{lcfs} \times \text{compression}_a \times \text{electricity} \times \text{q_captf}_c \Big\} + \\
& \sum_l \Big\{ (\text{ad}_l \times (\sum_{i=1}^{n} \vec{\mathbf{Intl}}_i)) + \\
& \vec{\mathbf{up_inj}} \times \text{q_ch4f}_l + \vec{\mathbf{comp_capt}} \times \text{q_captf}_l + \\
& \text{lcfs} \times \text{compression}_a \times \text{electricity} \times \text{q_captf}_l \Big\} + \\
& \sum_{s,f,t} \Big\{ (\text{fs_dist}_{s,f} \times \text{fs_mi} + \text{fs_time}_{s,f} * \text{fs_hr}) \times \frac{\text{q_feed}_{s,f,t}}{\text{fs_truckload}} + \\
& \text{per_ton}_{s,f} \times \text{q_feed}_{s,f,t} \Big\} + \\
& \sum_{f,i} \Big\{ (\text{rs_time}_{f,i} \times \text{rs_hr} + \text{rs_dist}_{f,i} \times \text{rs_mi}) \times \frac{\text{q_co2trans}_{f,i}}{\text{co2_truckload}} + \\
& \text{lcfs} \times \text{transport} \times \text{q_co2trans}_{f,i} \times \text{rs_dist}_{f,i} \Big\} + \\
& \sum_i \Big\{ (\text{seq}_i \times ((\text{injection_fc}_i + \text{seismic}_i) \times \text{crf} + \text{injection_vc}_i)) + \\
& \vec{\mathbf{comp_mon}} \times \text{q_co2seq}_i + \text{lcfs} \times \text{compression}_b \times \text{electricity} \times \text{q_co2seq}_i \Big\}
\end{aligned} \tag{4}$$

and total revenue is defined as:

$$\begin{aligned}\text{total revenue} = &\sum_{c}\Big\{\text{q\_ch4f}_c \times (\text{rng} + \text{d5})\Big\} + \sum_{l}\Big\{\text{q\_ch4f}_l \times (\text{rng} + \text{d5} + \text{cellulosic})\Big\} + \\ &\sum_{t,f}\Big\{\text{q\_ch4}_{t,f} \times [\text{lcfs} \times (\text{baseline\_ci} - \text{c\_intensity}_t)]\Big\} + \\ &\sum_{f}\Big\{\text{q\_captf}_f \times \vec{\mathbf{45q}}\Big\} + \\ &\sum_{i}\Big\{\text{q\_co2seq}_i \times (\text{lcfs})\Big\}\end{aligned} \tag{5}$$

We denote $\vec{\mathbf{Intc}}$ to be a vector of all piecewise intercepts relevant to the total costs for codigesting facilities and $\vec{\mathbf{Intl}}_l$ to be a vector of all piecewise intercepts relevant to the total costs for landfills:

$$\vec{\mathbf{Intc}} = \begin{bmatrix} \text{ad\_fc\_int} \times \text{crf} \\ \text{ad\_vc\_int} \\ \text{up\_fc\_int} \times \text{crf} \\ \text{up\_vc\_int} \\ \text{inj\_fc\_int} \times \text{crf} \\ \text{inj\_vc\_int} \\ \text{comp\_fc\_int}_a \times \text{crf} \\ \text{comp\_vc\_int}_a \\ \text{cap\_fc\_int} \times \text{crf} \\ \text{cap\_vc\_int} \\ \text{pipe\_fc}_c \times \text{crf} \\ \text{pipe\_vc}_c \end{bmatrix} \qquad \vec{\mathbf{Intl}} = \begin{bmatrix} \text{lmop}_l \\ \text{up\_fc\_int} \times \text{crf} \\ \text{up\_vc\_int} \\ \text{inj\_fc\_int} \times \text{crf} \\ \text{inj\_vc\_int} \\ \text{comp\_fc\_int}_a \times \text{crf} \\ \text{comp\_vc\_int}_a \\ \text{cap\_fc\_int} \times \text{crf} \\ \text{cap\_vc\_int} \\ \text{pipe\_fc}_l \times \text{crf} \\ \text{pipe\_vc}_l \end{bmatrix}$$

We denote $\vec{\mathbf{ad\_fc}}$ and $\vec{\mathbf{ad\_vc}}$ to be vectors of the piecewise slopes for fixed and variable costs for anaerobic digesters, taking on different values depending on the value of $\text{q\_feed}_{s,f,t}$.

$$\vec{\mathbf{ad\_fc}} = \begin{bmatrix} \text{ad\_fc\_slope}_1 \\ \text{ad\_fc\_slope}_2 \end{bmatrix} \times \text{crf} \qquad \vec{\mathbf{ad\_vc}} = \begin{bmatrix} \text{ad\_vc\_slope}_1 \\ \text{ad\_vc\_slope}_2 \end{bmatrix}$$

We denote $\vec{\mathbf{up\_inj}}$ and $\vec{\mathbf{comp\_capt}}$ to be vectors of the piecewise slopes for fixed and variable costs for upgrading and injection, and compression and CO_2 capture, respectively. Facilities take on different values within these vectors depending on the values of q_captf_f and q_ch4f_f.

$$\vec{\mathbf{up\_inj}} = \begin{bmatrix} (\text{up\_fc\_slope}_1 + \text{inj\_fc\_slope}_1) \times \text{crf} + \text{up\_vc\_slope}_1 + \text{inj\_vc\_slope}_1 \\ (\text{up\_fc\_slope}_2 + \text{inj\_fc\_slope}_2) \times \text{crf} + \text{up\_vc\_slope}_2 + \text{inj\_vc\_slope}_2 \end{bmatrix}$$

$$\vec{\mathbf{comp\_capt}} = \begin{bmatrix} (\text{comp\_fc\_slope}_{a1} + \text{capt\_fc\_slope}_1) \times \text{crf} + \text{comp\_vc\_slope}_{a1} + \text{capt\_vc\_slope}_1 \\ (\text{comp\_fc\_slope}_{a2} + \text{capt\_fc\_slope}_2) \times \text{crf} + \text{comp\_vc\_slope}_{a2} + \text{capt\_vc\_slope}_2 \end{bmatrix}$$

We denote $\vec{\mathbf{comp\_mon}}$ to be vectors of the piecewise slopes for fixed and variable costs of monitoring and compression cost at sequestration sites. Sequestration sites take on values within these vectors depending on the value of q_co2seq_i.

$$\vec{\mathbf{comp\_mon}} = \begin{bmatrix} \text{comp\_fc\_slope}_{b1} \times \text{crf} + \text{comp\_vc\_slope}_{b1} + \text{monitoring} \\ \text{comp\_fc\_slope}_{b2} \times \text{crf} + \text{comp\_vc\_slope}_{b2} + \text{monitoring} \end{bmatrix}$$

We denote $\vec{\mathbf{45q}}$ to be a vector of the piecewise values for the 45Q tax credits around the threshold of 100,000 tCO_2/year.

$$\vec{\mathbf{45q}} = \begin{bmatrix} 0 \\ 50 \end{bmatrix}$$

Constraints. The objective function is subject to:

Feedstock used is zero if the facility is not activated

$$\text{q\_feed}_{s,f,t} \leq \text{supply}_{s,t} \times \text{ad}_f \tag{6}$$

Feedstock used cannot exceed available supply

$$\sum_f \text{q\_feed}_{s,f,t} = \text{supply}_{s,t} \tag{7}$$

CO_2 transported is equal to CO_2 captured

$$\sum_i \text{q\_co2trans}_{f,i} = \text{q\_captf}_f \tag{8}$$

CO_2 sequestered is equal to CO_2 transported

$$\sum_f \text{q\_co2trans}_{f,i} = \text{q\_co2seq}_i \tag{9}$$

CO_2 sequestered cannot be more than available capacity

$$\text{q\_co2seq}_i \leq \text{capacity}_i \times \text{seq}_i \tag{10}$$

Minimum sequestration volume

$$\text{q\_co2seq}_i \geq 25000 \times \text{seq}_i \tag{11}$$

References

[1] CalFire. Incorporated cities. URL https://frap.fire.ca.gov/mapping/gis-data/. Accessed on 2020-08-01.

[2] Caltrans. City boundaries. URL https://gisdata-caltrans.opendata.arcgis.com/search?tags=Boundaries. Accessed on 2020-08-01.

[3] California geological survey, . URL https://www.conservation.ca.gov/cgs. Accessed on 2020-08-01.

[4] Hanna Marie Breunig, Tyler Huntington, Ling Jin, Alastair Robinson, and Corinne Donahue Scown. Temporal and geographic drivers of biomass residues in california. *Resources, Conservation and Recycling*, 139:287–297, 2018. ISSN 0921-3449. doi: 10.1016/j.resconrec.2018.08.022. URL http://www.sciencedirect.com/science/article/pii/S0921344918303148. Accessed on 2020-07-31.

[5] Filomena Ardolino and Umberto Arena. Biowaste-to-biomethane: An LCA study on biogas and syngas roads. *Waste Management*, 87:441–453, 2019. ISSN 0956-053X. doi: 10.1016/j.wasman.2019.02.030. URL http://www.sciencedirect.com/science/article/pii/S0956053X19301011. Accessed on 2020-08-01.

[6] Overview | places API, . URL https://developers.google.com/places/web-service/overview. Accessed on 2020-08-01.

[7] Daniel L. Sanchez, Nils Johnson, Sean T. McCoy, Peter A. Turner, and Katharine J. Mach. Near-term deployment of carbon capture and sequestration from biorefineries in the united states. *Proceedings of the National Academy of Sciences*, 115(19):4875–4880, 2018. ISSN 0027-8424, 1091-6490. doi: 10.1073/pnas.1719695115. URL https://www.pnas.org/content/115/19/4875. Accessed on 2020-07-31.

[8] National Energy Technology Laboratory. NATCARB/ATLAS, 2021. URL https://www.netl.doe.gov/coal/carbon-storage/strategic-program-support/natcarb-atlas. Accessed on 2020-08-01.

[9] J. Ogden and N. Johnson. Techno-economic analysis and modeling of carbon dioxide (CO2) capture and storage (CCS) technologies. In M. Mercedes Maroto-Valer, editor, *Developments and Innovation in Carbon Dioxide (CO2) Capture and Storage Technology*, volume 1 of *Woodhead Publishing Series in Energy*, pages 27–63. Woodhead Publishing, 2010. ISBN 978-1-84569-533-0. doi: 10.1533/9781845699574.1.27. URL http://www.sciencedirect.com/science/article/pii/B9781845695330500023. Accessed on 2020-08-01.

[10] Sean T. McCoy. The economics of CO2 transport by pipeline and storage in saline aquifers and oil reservoirs. 2009. doi: 10.1184/R1/6073547.v1. URL https://kilthub.cmu.edu/articles/journal_contribution/The_Economics_of_CO_sub_2_sub_Transport_by_Pipeline_and_Storage_in_Saline_Aquifers_and_Oil_Reservoirs/6073547. Accessed on 2020-08-01.

[11] Jan Martin Nordbotten, Michael A. Celia, and Stefan Bachu. Injection and storage of CO2 in deep saline aquifers: Analytical solution for CO2 plume evolution during injection. *Transport in Porous Media*, 58(3):339–360, 2005. ISSN 1573-1634. doi: 10.1007/s11242-004-0670-9. URL https://doi.org/10.1007/s11242-004-0670-9. Accessed on 2020-08-01.

[12] Ting Horng Chung, Mohammad Ajlan, Lloyd L. Lee, and Kenneth E. Starling. Generalized multiparameter correlation for nonpolar and polar fluid transport properties. *Industrial & Engineering Chemistry Research*, 1988. URL https://pubs.acs.org/doi/10.1021/ie00076a024. Accessed on 2020-08-01.

[13] Michael Batzle and Zhijing Wang. Seismic properties of pore fluids. *GEOPHYSICS*, 57(11):1396–1408, 1992. ISSN 0016-8033, 1942-2156. doi: 10.1190/1.1443207. URL http://library.seg.org/doi/10.1190/1.1443207. Accessed on 2020-08-01.

[14] David L. McCollum and Joan M. Ogden. Techno-economic models for carbon dioxide compression, transport, and storage & correlations for estimating carbon dioxide density and viscosity. 2006. URL https://escholarship.org/uc/item/1zg00532. Accessed on 2020-08-01.

[15] Nathan Parker, Robert Williams, Rosa Dominguez-Faus, and Daniel Scheitrum. Renewable natural gas in california: An assessment of the technical and economic potential. *Energy Policy*, 111:235–245, 2017. ISSN 0301-4215. doi: 10.1016/j.enpol.2017.09.034. URL http://www.sciencedirect.com/science/article/pii/S0301421517305955. Accessed on 2020-07-31.

[16] Peter C. Psarras, Stephen Comello, Praveen Bains, Panunya Charoensawadpong, Stefan Reichelstein, and Jennifer Wilcox. Carbon capture and utilization in the industrial sector. *Environmental Science & Technology*, 51(19):11440–11449, 2017. ISSN 1520-5851. doi: 10.1021/acs.est.7b01723.

[17] Gray Davis. Economic and financial aspects of landfill gas to energy project development in california, 2002.

[18] P. W. Tittmann, N. C. Parker, Q. J. Hart, and B. M. Jenkins. A spatially explicit techno-economic model of bioenergy and biofuels production in california. *Journal of Transport Geography*, 18(6):715–728, 2010. ISSN 0966-6923. doi: 10.1016/j.jtrangeo.2010.06.005. URL http://www.sciencedirect.com/science/article/pii/S0966692310000864. Accessed on 2020-07-31.

[19] Yeqing Li, Ruihong Zhang, Guangqing Liu, Chang Chen, Yanfeng He, and Xiaoying Liu. Comparison of methane production potential, biodegradability, and kinetics of different organic substrates. *Bioresource Technology*, 149:565–569, 2013. ISSN 0960-8524. doi: 10.1016/j.biortech.2013.09.063. URL http://www.sciencedirect.com/science/article/pii/S0960852413014958. Accessed on 2020-07-31.

[20] Humberto Escalante, Liliana Castro, Paola Gauthier-Maradei, and Reynel Rodríguez De La Vega. Spatial decision support system to evaluate crop residue energy potential by anaerobic digestion. *Bioresource Technology*, 219:80–90, 2016. ISSN 0960-8524. doi: 10.1016/j.biortech.2016.06.136. URL http://www.sciencedirect.com/science/article/pii/S0960852416309609. Accessed on 2020-08-01.

[21] California Department of Food {and} Agriculture. Agricultural overview. URL http://www.cdfa.ca.gov/Statistics/PDFs/AgResourceDirectory2008/1_2008_OverviewSection.pdf. Accessed on 2020-08-01.

[22] California Air Resources Board. Low carbon fuel standard amendments. 2019. URL https://ww2.arb.ca.gov/rulemaking/2019/lcfs2019. Accessed on 2020-08-01.

[23] OAR US EPA. Emissions & generation resource integrated database (eGRID), 2015. URL https://www.epa.gov/energy/emissions-generation-resource-integrated-database-egrid. Accessed on 2020-08-01.

[24] Environmental Defense Fund. Green freight math: How to calculate emissions for a truck move. URL https://business.edf.org/insights/green-freight-math-how-to-calculate-emissions-for-a-truck-move/. Accessed on 2020-08-01.

[25] Qie Sun, Hailong Li, Jinying Yan, Longcheng Liu, Zhixin Yu, and Xinhai Yu. Selection of appropriate biogas upgrading technology-a review of biogas cleaning, upgrading and utilisation. *Renewable and Sustainable Energy Reviews*, 51:521–532, 2015. ISSN 1364-0321. doi: 10.1016/j.rser.2015.06.029. URL http://www.sciencedirect.com/science/article/pii/S1364032115006012. Accessed on 2020-07-31.

[26] Matthew D Ong, Robert B Williams, and Stephen R Kaffka. Comparative assessment of technology options for biogas clean-up. page 161, 2014. URL https://biomass.ucdavis.edu/files/2015/10/Biogas-Cleanup-Report_FinalDraftv3_12Nov2014-2.pdf. Accessed on 2020-07-30.